IEEE Access
Multidisciplinary | Rapid Review | Open Access Journal

Received April 23, 2021, accepted April 26, 2021, date of current version May 18, 2021.

Digital Object Identifier 10.1109/ACCESS.2021.3078585

Enhanced Computational Intelligence Algorithm for Coverage Optimization of 6G Non-Terrestrial Networks in 3D Space

MOHAMED ABDEL-BASSET, LAILA ABDEL-FATAH, KHALID A. ELDRANDALY, AND NABIL M. ABDEL-AZIZ

Faculty of Computers and Informatics, Zagazig University, Sharqiyah 44519, Egypt

Corresponding author: Laila Abdel-Fatah (englaila2013@gmail.com)

ABSTRACT The next generation 6G communication network is typically characterized by the full connectivity and coverage of Users Equipment (UEs). This leads to the need for moving beyond the traditional two-dimensional (2D) coverage service to the three-dimensional (3D) full-service one. The 6G 3D architecture leverages different types of non-terrestrial or aerial nodes that can act as mobile Base Stations (BSs) such as Unmanned Aerial Vehicles (UAVs), Low Altitude Platforms (LAPs), High-Altitude Platform Stations (HAPSs), or even Low Earth Orbit (LEO) satellites. Moreover, aided technologies have been added to the 6G architecture to dynamically increase its coverage efficiency such as the Reconfigurable Intelligent Surfaces (RIS). In this paper, an enhanced Computational Intelligence (CI) algorithm is introduced for optimizing the coverage of UAV-BSs with respect to their location from RIS in the 3D space of 6G architecture. The regarded problem is formulated as a constrained 3D coverage optimization problem. In order to increase the convergence of the proposed algorithm, it is hybridized with a crossover operator. For the validation of the proposed method, it is tested on different scenarios with large-scale coordinates and compared with many recent and hybrid CI algorithms, as Slime Mould Algorithm (SMA), Lévy Flight Distribution (LFD), hybrid Particle Swarm Optimization and Gravitational Search Algorithm (PSOGSA), the Covariance Matrix Adaptation Evolution Strategy (CMA-ES), and hybrid Grey Wolf Optimizer and Cuckoo Search (GWOCS). The experiment and the statistical analysis show the significant efficiency of the proposed algorithm in achieving complete coverage with a lower number of UAV-BSs and without constraints violation.

INDEX TERMS 6G technology, computational intelligence, non-terrestrial base stations, reconfigurable intelligent surfaces, three-dimensional coverage optimization problem.

I. INTRODUCTION

Roughly speaking, the usage of fifth-generation (5G) technology is adequate for the current demand of several countries. This is because 5G technology preserves internet protocol television, high-definition video streaming, basic virtual and augmented reality services, and faster transmission. However, it is an urgent issue to shift to another extensive networking technology because of the exponential increase of Internet of Things (IoT) objects and their related flood of user-centric information. In particular, the expected number of IoT-connected objects will be 41.6 billion in 2025 according to International Data Corporation (IDC). Moreover, by the 2040s, it is expected that the number of IoT-connected objects will reach trillions according to IEEE Conference on Standards for Communications and Networking (CSCN) [1].

The vision of sixth-generation (6G) technology has begun with the aim of providing telecommunications services for future requirements over the upcoming years that is expected to reach huge data rates up to 1 Tb/s and wide-ranging frequency bands of 100 GHz to 3 THz. As shown in Fig.1, 6G technology is a full-scale on-demand self-reconfiguration wireless network that envisaged to incorporate advanced features with existing 5G technology to meet high-rate individual and commercial demands. There are many services added by 6G technologies, such as Artificial Intelligence (AI), holographic communications, high precision manufacturing,

The associate editor coordinating the review of this manuscript and approving it for publication was Yudong Zhang.

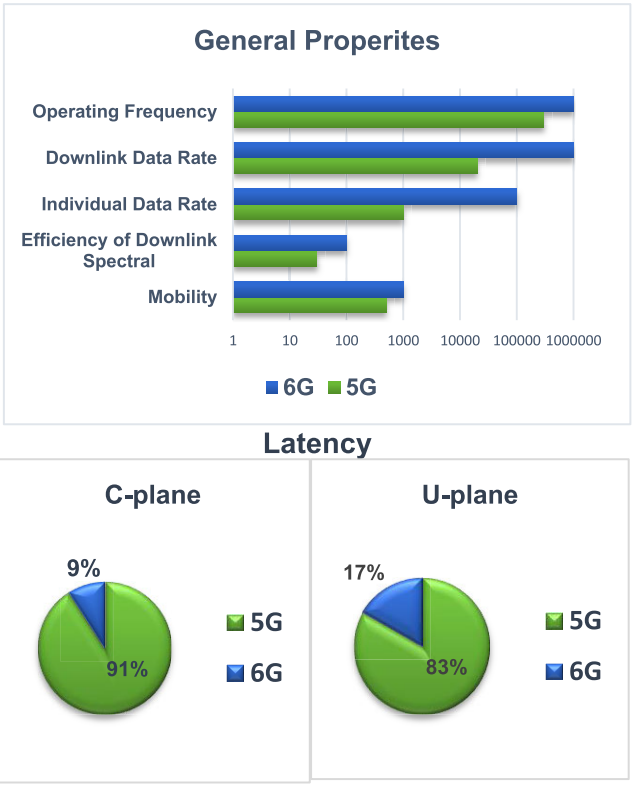

FIGURE 1. 6G verses 5G.

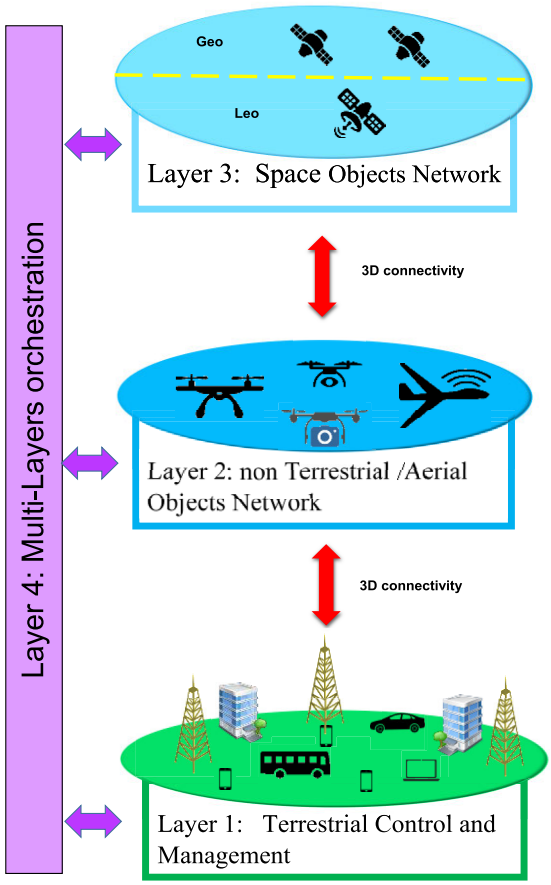

FIGURE 2. 3D layers of 6G technology.

Visible Light Communications (VLC), terrestrial, aerial radio APs for cloud services, and three-dimensional (3D) coverage framework.

The 3D full coverage of 6G technology obligates shifting from the standard hierarchy and specifications. Accordingly, the standards of the 3rd Generation Partnership Project (3GPP) will be appropriate for these interfered network components. Each non-terrestrial node has its own specific features as altitude, payload, computation latency, storage, coverage area, and so on. As shown in Fig.2, the 3D hierarchy of 6G technology contains various aerial objects in each networking layer, such as Unmanned Aerial Vehicles (UAVs), Low Altitude Platforms (LAPs), High-Altitude Platform Stations (HAPSs), and Even Low Earth Orbit (LEO) satellites. The cooperation of these flying objects can be utilized to deliver unified and affordable high-level Quality of Services (QoS) to Users Equipment (UEs) especially for remote areas and emergency scenarios [2]. Another great advantage of the 3D architecture of 6G technology is that it can be leveraged to increase the connectivity and reliability of the two-dimensional (2D) plane besides its comprehensive 3D networking services.

Unmanned Aerial Vehicle Base Stations (UAV-BSs) are mobile base stations with an unprecedented degree of freedom which makes them work in the low-frequency, microwave, and mm-wave bands. These features provide more flexible and reliable connectivity and on-demand time- and spatially-varying services. Therefore, UAV-BSs offer jointly real-time control and computation with complete services in 3D space. With AI guidance, UAV-BSs can be dynamically reallocated to prevent interference and increase area coverage.

Reconfigurable Intelligent Surfaces (RIS) or what so-called Intelligent Reflecting Surfaces (IRS) have led to the emergence of the "smart radio environments" concept. In particular, RIS affords auto-configuration of reflecting electromagnetic waves propagation environment from meta-surfaces by electronic devices like pin-diodes or varactors. As mentioned above, the full coverage feature of 6G technology leads to the exploitation of additional coverage increment methods. As a consequence, RIS has become an integral part of any 6G system. In other words, it can be considered a 6G sub-technology [3].

AI is a key feature in 6G technology and it plays an important role in the 6G communication revolution. For instance, AI-based algorithms or so-called Computational Intelligence (CI) algorithms can be used for network resource allocation and smart management of the spectrum in order to attain close-to-optimum performance. Also, they can be used for realizing the environment and applying a real-time adjustment to radio waves.

In this paper, an enhanced CI algorithm called "Marine Predators Algorithm with Crossover (CMPA)" is proposed to

maximize the coverage of 6G technology by finding the best positions of UAV-BSs and RIS. This problem is formulated as a constrained 3D coverage optimization problem. The proposed algorithm proves its efficiency in achieving ubiquitous coverage without constraint violations.

The rest of this paper is organized as follows: Section 2 presents a literature review of the related works, section 3 describes the considered 6G system configurations, the definition of the constraint 3D coverage problem is introduced in section 4, the proposed algorithm is introduced in section 5, the validation experiment is conducted in section 6, the implication of the proposed algorithm on cost-efficient QoS of 6G technology is discussed in section 7, and finally the conclusion and future works are given in section 8.

II. LITERATURE REVIEW

Because the 6G technology is still emerging in lots of countries, the literature that discusses 6G optimization is relatively few. Fig.3 shows the percentages of published literature that handle the 6G-related topics from 2016 to 2020 (forecast from Scopus, Google scholar, and IEEE explore). As observed, the literature that handling the optimization of 6G is very few. Regarding the 6G coverage optimization, the related literature is almost scarce. Next, the most recent examples of literature that handling 6G optimization and the 3D coverage optimization will be presented.

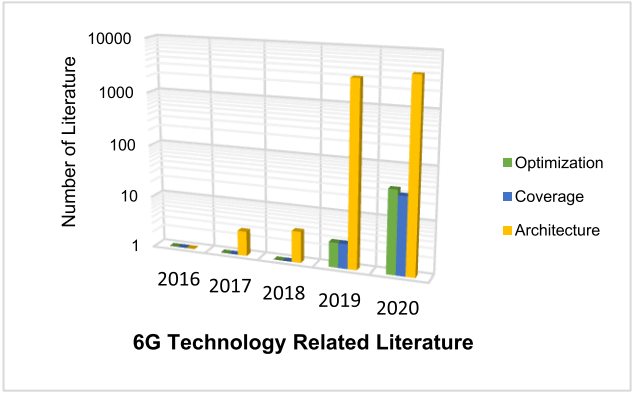

FIGURE 3. 6G related literature (Forecast).

A. THE LITERATURE OF 6G OPTIMIZATION

Nawaz *et al.* [4] introduced a Quantum Machine Learning (QML) based framework for the communication of 6G wireless networks. The proposed framework was able to blend the intelligence with various 6G levels of architecture, as network-infrastructure, network-edge, proactive caching, multi-objective routing optimization, resource allocation, big data analytics, and mmWave communications, etc. However, the role of CI algorithms was not addressed in this literature. Also, there were no conducted experiments or statistical comparisons.

Letaief *et al.* [5] proposed a roadmap of the possible usage of AI in optimizing the performance of 6G wireless systems. The authors suggested applying AI-based optimization to the analytics of 6G big data, closed-loop, and wireless communication. Also, Yang *et al.* [6] discussed the potentials of AI usage in the layers' optimization of 6G technology. The authors showed that the architecture of 6G consists of four main layers, including intelligent sensing, data mining and analytics, intelligent control, and smart application layers. In addition, AI leverages in each layer were discussed.

Hashida *et al.* [7] presented the problem of RIS placement optimization. The authors discussed the effect of Base Stations (BSs) and RIS positions on communication with Aerial Users (AUs). The main objective of this optimization problem is to maximize the spatial signal-to-interference-plus-noise ratio (SINR) while mitigating inter-cell interference. Although the authors proposed the optimal placement of RIS for the best coverage of AUs, they didn't point out the placement of BSs. Also, Hashida *et al.* didn't use any optimization algorithms for finding the best placement of RIS.

Fu *et al.* [8] introduced an AI-based framework of 6G Recommendation-aware Content Caching (RCC). On the other hand, the authors introduced a general framework without studying the performance of a specific optimization algorithm. In addition, the authors didn't mention the coverage issue of the 6G technology.

Tarable *et al.* [9] introduced a mathematical model for the pre-configuration of 6G meta-surface orientation. The main objective of the proposed mathematical model is the optimization of sub-Terahertz (sub-THz) wireless networks in the 6G technology environment. However, the authors didn't mention the roles of AI techniques and only mention one heuristic optimization technique in the optimization of sub-THz wireless networks.

Regarding the resource allocation of 6G networks, Yu *et al.* [10] used the Greedy Shrinking Algorithm (GSA) for the Joint Time-Slot and Sub-band scheduling and Power (JTSP) allocation problem. The proposed problem was expressed in the form of a Mixed-Integer Nonlinear Programming (MINLP) problem. The proposed scheme achieved a 12.5% to 60.7% increase in productivity. Also, Calvanese Strinati *et al.* [11] proposed an overview and modeling of the resource allocation of interfered flying devices in the 3D environment. The authors didn't handle the coverage issue of the 6G networks in the 3D environment.

B. THE LITERATURE OF 3D COVERAGE OPTIMIZATION

Watfa and Commuri [12] introduced an analysis of the 3D coverage problem. They proposed an algorithm for distributing sensors in areas with small dimensions.

The authors in [13] proposed two different appointments of sensors in the 3D regions. These static arrangements preserved the connectivity between sensors and area coverage.

Andersen and Tirthapura [14] presented a discrete formulation of a 3D coverage problem that can reduce the number of needed sensors.

Liu *et al.* [15] proposed the Artificial Fish Swarm Algorithm (AFSA) for 3D coverage for healthcare purposes and applied it for only one observed area.

Sharma and Gupta [16] proposed a multi-objective formulation of a 3D coverage problem. This multi-objective function comprised the distance metric between double sensors and the used ones. The Harmony Search (HS) algorithm was used for solving this multi-objective problem. Besides, the authors deployed the proposed technique to increase the performance of a network lifetime. Comparing to the Low-Energy Adaptive Clustering Hierarchy (LEACH) protocol, it has a good performance. On the other hand, the main disadvantage of the proposed technique was the incomplete coverage of the observed area.

Ding *et al.* [17] presented the Fuzzy Harris hawks optimizer (FHHO) for 3D monitoring of cardiomyopathy patients. In addition, the authors proposed the Wearable Sensing Data Optimization (WSDO) algorithm for precise and consistent cardiomyopathy sensing data manipulation.

C. THE CONTRIBUTIONS OF THIS LITERATURE

This work introduces an enhanced CI algorithm for leveraging the coverage of 6G networks in the 3D environment. In particular, Marine Predators Algorithm (MPA) [18] is chosen for handling the regarded problem due to several reasons which are scalability, rapidness, high-quality solutions, and a good exploration of the search space as it comprises several distributions while searching (as we will discuss next).

From the above-discussed kinds of literature, there was no literature handling the problem of allocation of UAV-BSs with respect to RIS using CI algorithms [19]. In other words, the previously proposed methods are limited to machine learning methods, theoretical frameworks, and mathematical representation. On the other hand, the used CI algorithms proposed for the 3D coverage optimization problem also didn't address the optimization problem of UAV-BSs allocation with respect to RIS.

III. PROBLEM DESCRIPTION

RIS is a full-duplex transparent rebroadcast technology that simultaneously receives the signal from transmitters and then re-radiates the propagation of the radio waves impinging upon it with controllable time-delays [20]. RIS comprises many nanoengineered structures (reflecting elements, equivalent circuits, and controllers, etc.) that can set different time delays, thus aggregating the scattering behavior of an arbitrarily shaped object of the same size. These semi-passive elements on the RIS reflect the impinged signal with adjustable phase shift and without the need for a dedicated power source for signal processing, making it highly energy-efficient [21].

In particular, RIS is constructed from small, lightweight, and compatibility elements that are attached to a low profile surface. As a consequence, it can be easily deployed on objects with high elevation in order to enhance transmission strength with beamforming and the use of multipath (such as facades of buildings, factory walls, ceilings, and billboards). Moreover, RIS offers channel optimization besides the optimization of transmitter and receiver. This provides a transformative medium for a naturally passive wireless environment into a programmable smart entity. RIS can be easily integrated into existing wireless networks without the modification of its uniformity of the physical layer, making it transparent to users. Therefore, consideration must be given to the place of BSs instruction with respect to the angle of incidence on the RIS because it greatly affects the reflected electromagnetic waves. In general, the static physical structure of RIS makes it preferable to exploit a mobile BS to support propagated signals such as UAV-BSs.

This paper deals with the allocation of UAV-BSs in order to increase the coverage percentage as well as consider the incident angle on the RIS.

IV. PROBLEM MATHEMATICAL FORMULATION

In this section, the positioning problem of RIS-empowered UAV-BSs is formulated as a constraint 3D coverage optimization problem. Next, we will discuss all related definitions.

A. 3D COVERAGE MODEL

Let $\boldsymbol{S}$ be a set of $\boldsymbol{k}$ UAV-BSs such that $\boldsymbol{S} = \{\boldsymbol{s_1}\, \boldsymbol{s_2}, \ldots, \boldsymbol{s_k}\}$. Each $\boldsymbol{s_k}$ has a sphere-shaped wave with a radius $\boldsymbol{r_k}$. As well, each $\boldsymbol{s_k}$ has a coordinate $(\boldsymbol{x_k}, \boldsymbol{y_k}, \boldsymbol{z_k})$ in the 3D plane. Accordingly, the area covered by a spherical wave can be computed as:

$$Cov_k = \frac{4\pi r_k^3}{3} \tag{1}$$

where Cov_k is the sphere-shaped coverage zone of a UAV-BS k.

B. 3D COVERAGE PERCENTAGE

The 3D covered area called A is partitioned into discrete points $a(x, y, z)$ where any point $a(x, y, z)$ is covered by a UAV-BS s_k if the Euclidean distance between s_k and p is smaller than the sphere-shaped coverage radius r_k, as:

$$d\,(a, s_k) = \sqrt{(x - x_k)^2 + (y - y_k)^2 + (z - z_k)^2} \tag{2}$$

So, the coverage percentage of a set of UAV-BSs can be computed via dividing the covered points by the total points of the area to be covered as:

$$\mathrm{Z} = \frac{\|a^c\|}{\|a\|} \tag{3}$$

where a^c is a covered point and a is any point in the 3D area to be covered.

C. THEORETICAL 3D COVERAGE PERCENTAGE

Formerly, the theoretical 3D coverage percentage of $\boldsymbol{k}$ UAV-BSs can be calculated as [15]:

$$X = 1 - \left(1 - \frac{4\pi r_k^3}{3L}\right)^k \tag{4}$$

where L is the volume of the area to be covered, and X is the theoretically expected coverage ratio.

Thence, the corresponding number of UAV-BSs that attains X coverage percentage can be computed as [17]:

$$\tilde{k} = \frac{\ln(1-X)}{\ln\left(1 - \frac{4\pi r_{\tilde{k}}^3}{3L}\right)} \tag{5}$$

where $\tilde{k}$ is the corresponding number of UAV-BSs and $r_{\tilde{k}}$ is the predefined coverage radius of a UAV-BS $\tilde{k}$.

D. FORMULATION OF OPTIMIZATION PROBLEM

In this paper, the area to be covered is divided by a virtual 3D grid, then the resultant grid points are calculated. Thence, the 3D coverage optimization problem can be formulated as:

$$\begin{aligned} &\max f = \frac{\sum_{j=1}^{w} x_j}{G} \\ &\textbf{\textit{subject to}} \quad \boldsymbol{x_j \leq G}, \\ &x_j = \begin{cases} \mathbf{1}, & \textbf{if a } \boldsymbol{g} \textbf{ point is covered} \\ \mathbf{0}, & \textbf{Otherwise} \end{cases} \quad , \boldsymbol{g} \in G \end{aligned} \tag{6}$$

where $\boldsymbol{w}$ is the total number of UAV-BSs, $\boldsymbol{G}$ is the total number of calculated grid points and $\boldsymbol{x_j}$ is a binary variable indicated whether a grid point g is covered or not.

E. SPATIAL ALLOCATION OF UAV-BSS WITH RIS

The RIS empowered propagation is more vital than increasing the number of used BSs because it can decrease the imperfections of various propagation environments and fade the coverage holes. The spatial allocation of RIS and UAV-BSs effects on the 6G coverage. In particular, there are three main links in any RIS-empowered UAV-BSs, including UAV-BSs to the user, RIS to the user, and RIS to UAV-BSs. The first link is the direct link that connected UAV-BSs with a user. The second link represents the connections between RIS and a user. The last link demonstrates the link between RIS and UAV-BSs. In the 3D space, the incident angle from UAV-BSs determines the direction of the reflected waves from RIS. So that, it can mainly affect the coverage of the whole 6G system. In addition, the distance between UAV-BSs and RIS must have a predetermined upper and lower bound. In this paper, not only UAV-BSs must be allocated at a certain angle and distance from RIS but also the coverage must be maximized without constraints violation.

V. PROPOSED ALGORITHM

In this section, the proposed enhanced technique for solving the 3D coverage is presented as shown in Fig.4.

A. MARINE PREDATORS ALGORITHM

The main inspiration of MPA is the biological interaction between hunter and victim in the marine environment. This interaction behavior mainly depends on Lévy and Brownian distribution behavior. The main governing assumptions of MPA are:

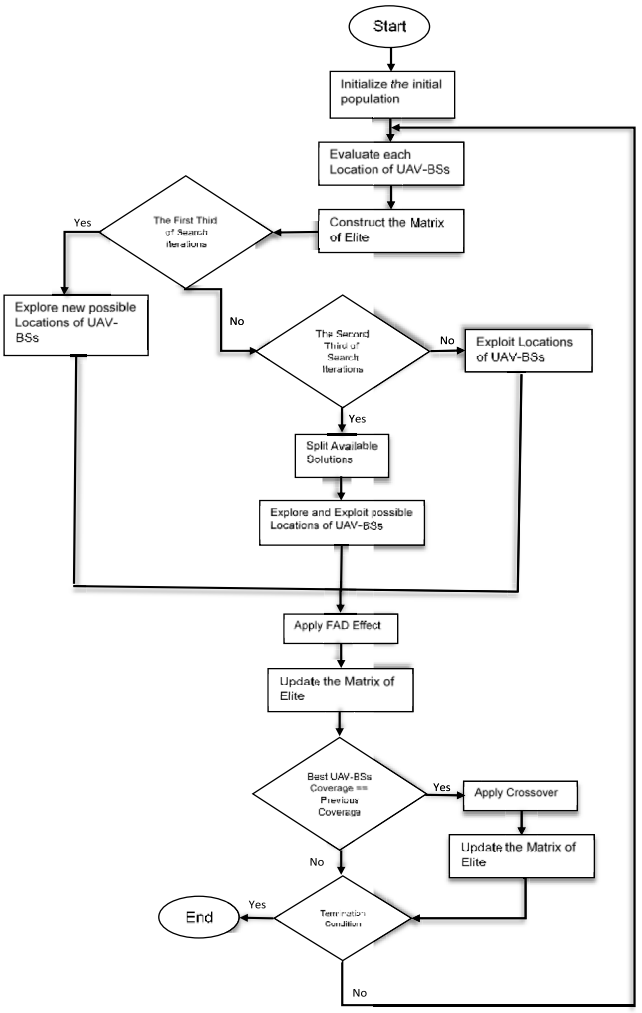

FIGURE 4. Flowchart of proposed allocation technique.

- Hunter or predators use the Lévy movement for the areas with a low intensity of victim and Brownian motion for the environment with the plentiful victim.
- The Lévy and Brownian motion percentages are the same.
- The behavior of a predator changes according to two factors natural eddy formation or human-caused (FADs).
- The best movement for a predator is Lévy's strategy in the low-Velocity ratio (V = 0.1) while the movement of the prey is either Brownian or Lévy.
- The best movement for a hunter is the Brownian strategy if a prey moves in Lévy in the case of the unit Velocity ratio (V = 1). The other cases depend on system size.
- The best movement for a hunter is not transferring at all while the prey is transferring either Brownian or Lévy in the high-Velocity ratio (V >= 10).
- In the high-velocity ratio, the prey utilizes best memory in the recapping of their associates and the best foraging location.

As MPA is a population-based metaheuristic, it begins with the random initialization of the starting population. After the

initialization step, the obtained solutions are ordered according to their fitness in order to construct the matrix of elite. This matrix contains the best solution or top hunter which is repeated n times where n is the population size. At the end of each search iteration, the matrix of elite is updated with a better predator. Besides, another matrix of prey is created with the same size as the matrix of elite. This matrix is responsible for updating the movement of the elite predator. In particular, the searching process of MPA consists of three main phases according to the level of the velocity ratio. In the first searching phase, the hunter is not transferring at all while the prey is transferring either Brownian or Lévy at the premature phase of searching (in the first third of total searching iterations) or with a high-velocity ratio (V >= 10). This is done by the following:

$$\overrightarrow{step_i} = \overrightarrow{R_B} \otimes \left(\overrightarrow{elite_i} - \overrightarrow{R_B} \otimes \overrightarrow{prey_i}\right) \quad i = 1, 2, \ldots, n \tag{7}$$

$$\overrightarrow{prey_i}(t+1) = \overrightarrow{prey_i}(t) + P.\overrightarrow{R} \otimes \overrightarrow{step_i} \tag{8}$$

where $\overrightarrow{step_i}$ is the prey step size, $\overrightarrow{R_B}$ is a vector of Brownian random numbers, the notation $\otimes$ means entry-wise multiplications, $\overrightarrow{elite_i}$ is the best predator from the matrix of elite, $\overrightarrow{prey_i}$ is a solution from the matrix of prey, P is a constant number, and $\overrightarrow{R}$ is a vector of uniform random numbers between [0, 1].

The second phase of searching happens in the second third of the total searching iterations. The best movement for a predator is the Brownian strategy if a prey moves in Lévy in the case of V = 1. Particularly, the population of search agents is divided into two subpopulations. The first half is updated as follows:

$$\overrightarrow{step_i} = \overrightarrow{R_L} \otimes \left(\overrightarrow{elite_i} - \overrightarrow{R_L} \otimes \overrightarrow{prey_i}\right) \quad i = 1, 2, \ldots, {}^{n}/_{2} \tag{9}$$

$$\overrightarrow{prey_i}(t+1) = \overrightarrow{prey_i}(t) + P.\vec{R} \otimes \overrightarrow{step_i} \tag{10}$$

where $\overrightarrow{R_L}$ is a vector of Lévy random numbers.

The second half of the population search agents is updated as follows:

$$\overrightarrow{step_i} = \overrightarrow{R_B} \otimes \left(\overrightarrow{R_B} \otimes \overrightarrow{elite_i} - \overrightarrow{prey_i}\right) \quad i = \frac{n}{2} + 1, \ldots, n \tag{11}$$

$$\overrightarrow{prey_i}(t+1) = \overrightarrow{elite_i} + P.C \otimes \overrightarrow{step_i} \tag{12}$$

where C is an adaptive parameter that calculated as:

$$C = \left(1 - \frac{it}{itmax}\right)^{\left(2 * \frac{it}{itmax}\right)} \tag{13}$$

where it is the current iteration number and $itmax$ is the maximum number of iterations.

The third phase of searching occurs in the last third of the total searching iterations. The best movement for a predator is Lévy's strategy (V = 0.1) while the movement of the prey is either Brownian or Lévy. The candidate solutions are updated as:

$$\overrightarrow{step_i} = \overrightarrow{R_L} \otimes \left(\overrightarrow{R_L} \otimes \overrightarrow{elite_i} - \overrightarrow{prey_i}\right) \quad i = 1, 2, \ldots, n \tag{14}$$

$$\overrightarrow{prey_i}(t+1) = \overrightarrow{elite_i} + P.C \otimes \overrightarrow{step_i} \tag{15}$$

Another searching mechanism is added to MPA which simulates natural eddy formation or FADs. The occurrence of such a case happens according to a predefined probability FADs which is set to 0.2. Then, the calculation of candidate solutions will be as follows:

$$\overrightarrow{prey_i}(t+1) = \begin{cases} \overrightarrow{prey_i}(t) + C\left[\overrightarrow{lb} + \overrightarrow{R} \otimes \left(\overrightarrow{ub} - \overrightarrow{lb}\right)\right] \otimes \vec{U}, & \text{if } rand \leq \text{FADs} \\ \overrightarrow{prey_i}(t) + [\text{FADs}\,(1 - \text{rand}) + \text{rand}]\left(\overrightarrow{prey_{r1}} - \overrightarrow{prey_{r2}}\right), & \text{otherwise} \end{cases} \tag{16}$$

where $\overrightarrow{lb}$ and $\overrightarrow{ub}$ are the vectors of the lower and upper bound of the searching domain, respectively, $\vec{U}$ is a random vector of binary numbers, $rand$ is a uniform random number between [0, 1], and $\overrightarrow{prey_{r1}}$ and $\overrightarrow{prey_{r2}}$ are two random preys. Algorithm 1. shows the MPA pseudo-code.

Algorithm 1 MPA Pseudo-Code

```
Set MPA parameters: itmax, n, FADS, P.
Initialize the initial population of preys i = 1, 2, ... n
while (it ≤ itmax) do
    Evaluate each prey
    Construct the matrix of elite
    if (it < itmax/3) then
        Exploration with high-velocity ratio of the prey
    elseif (itmax/3 < it < 2 * itmax/3) then
        Split the population of preys
        Intermittent search between exploration
        and exploitation
    else
        Exploitation with predator Lévy's movement
    endif
    Applying FADs Effect
    Update the matrix of elite
endwhile
return the best solution
```

B. CROSSOVER PHASE

For increasing the convergence of MPA, the crossover phase can be added. It allows the mixing of characteristics from various search agents in order to have a new search agent that owns good features from its predecessors. In this paper, the phase of crossover takes the generated solution which makes the elite solution unchanged the best search

agent (see Fig.4). This additional phase creates a new search agent as follows:

$$\overrightarrow{prey}_i(t+1) = \gamma .* \overrightarrow{elite}_i + (1-\gamma) .* \overrightarrow{\text{prey}^{\text{u}}} \quad (17)$$

where γ is a uniform random number between [0, 1] and $\overrightarrow{\text{prey}^{\text{u}}}$ is the generated solution that doesn't increase the fitness of the best solution. The pseudo-code of the proposed Marine Predators Algorithm with Crossover (CMPA) is represented in Algorithm 2.

C. HANDLING CONSTRAINTS

As shown in Fig.5, the regarded problem of 3D allocation of RIS empowered UAV-BSs has various constraints that should be handled. The first constraint is the incident angle between RIS and UAV-BSs. Typically, UAV-BSs rise at high altitudes while RISs are usually located on the building facade [22]. As a consequence, we assume in this paper that the incident angle is between [30], [50] degrees.

The second constraint is that the RIS must be connected to at least one UAV-BSs. The last constraint is that the distance between RIS and UAV-BSs must be greater than half of the UAV-BSs coverage radius.

In this paper, the Death Penalty method [23] is chosen for handling the previous constraints as it has lower complexity and simpler to be implemented. The Death Penalty method works based on the subtraction of a great number from the value of solution fitness in case of infeasibility. As a consequence, the infeasible solution is discarded from the candidate solutions.

VI. VALIDATION EXPERIMENT

A. EXPERIMENT SETUP

In order to validate the performance of the proposed algorithm, two validation experiments are conducted. In the first experiment, CMPA is tested on the allocation of UAV-BSs for only maximizing the area coverage. It is compared with several other CI algorithms, including Coyote Optimization Algorithm (COA) [24], Harris Hawks Optimization (HHO) [25], Slime Mould Algorithm (SMA) [26], Lévy Flight Distribution (LFD) [27], Salp Swarm Algorithm (SSA) [28], and Whale Optimization Algorithm (WOA) [29].

Moreover, the proposed algorithm is tested on the allocation of UAV-BSs with the previously mentioned constraints. In this experiment, CMPA is compared with two hybrid CI algorithms, including hybrid Particle Swarm Optimization and Gravitational Search Algorithm (PSOGSA) [30], the Covariance Matrix Adaptation Evolution Strategy (CMA-ES) [31], hybrid Grey Wolf Optimizer and Cuckoo Search (GWOCS) [32].

The used parameters of all comparators are listed in Table 1. The number of iterations is set to 150 for all algorithms. The population size is set to 10 except the population size of CMA-ES is computed according to the problem instant dimension, as:

$$Np = (4 + \lceil 3 \log(\dim) \rceil)^{10} \quad (18)$$

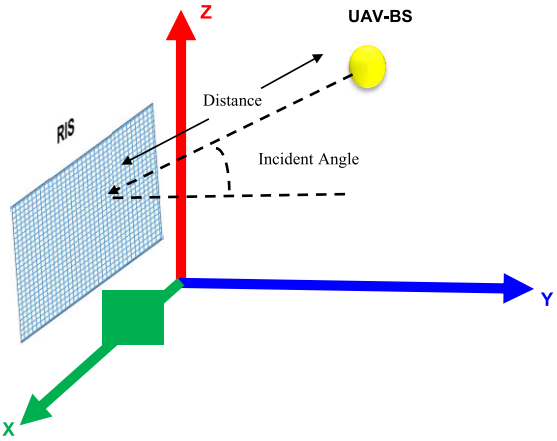

FIGURE 5. 3D RIS empowered UAV-BSs paradigm.

Algorithm 2 CMPA Pseudo-Code

```
Set MPA parameters: itmax, n, FADS, P.
Initialize the initial population of preys i = 1, 2, ... n
while (it ≤ itmax) do
    Calculate the coverage percentage f for each prey
    Construct the matrix of elite
    if (it < itmax/3) then
        Exploration with high-velocity ratio of the prey
    elseif (itmax/3 < it < 2 * itmax/3) then
        Split the population of preys
        Intermittent search between exploration and exploitation
    else
        Exploitation with predator Lévy's movement
    endif
    Applying FADs Effect
    Update the matrix of elite
    if still as previous then
        Apply crossover phase
        Update the matrix of elite
    endif
endwhile
return the best solution
```

where *Np* is the population size and dim is the dimension of the problem.

The experiments are carried out and all yalgorithms are coded in MATLAB R2020a. The device specifications are a 64-bit operating system with a 2.60 GHz CPU and 6 GB RAM.

B. LARGE-SCALE TEST CASES

The QoS of 6G wireless networks mainly depends on the coverage of vast areas. As a consequence, the validation test cases are generated in 3D large-scale coordinates ranging from 150 to 1,000 cubic meters for the first validation experiment. Table 2 shows the characteristics of the generated large-scale test cases for the first experiment. While the

TABLE 1. The parameters values of compared algorithms.

Algorithm	Parameters	Value
CMPA	Fish Aggregating Devices (FADs)	0.2
	P Constant	0.5
COA	Number of packs	1
HHO	Switching Probability	0.5
SMA	Switching Probability (z)	0.03
LFD	Switching Probability	0.5
SSA	Switching Probability	0.5
WOA	Switching Probability	0.5
PSOGSA	gravitational constant	1
	Acceleration coefficient C1	0.5
	Acceleration coefficient C2	1.5
CMA-ES	Coefficient alpha	2

TABLE 2. Characteristics of the first experiment large-scale test cases.

Cases	Large Scale Coordinates	UAV-BSs Numbers	Radius of Coverage	Expected coverage
Case 1	150 X 150 X 150	10	50	81%
Case 2	300 X 300 X 300	60	50	69%
Case 3	400 X 400 X 400	70	70	80%
Case 4	600 X 600 X 600	80	100	79%
Case 5	1000 X 1000 X 1000	100	150	80%

TABLE 3. Characteristics of the second experiment large-scale test cases.

Cases	Large Scale Coordinates	UAV-BSs Numbers	RIS Numbers	Radius of Coverage	Expected coverage
Case R1	1000 X 1000 X 1000	2	6	500	89.18 %
Case R2	1500 X 1500 X 1500	10	20	500	81.47 %
Case R3	2000 X 2000 X 2000	15	30	500	63.77 %

3D large-scale coordinates ranging from 1000 to 2000 for the second validation experiment. In Table 3, the characteristics of the generated large-scale test cases for the second experiment are presented.

C. HANDLING CONSTRAINTS

In this subsection, CMPA is tested on the large-scale test cases against the other comparators. For a fair comparison, each algorithm runs for 30 independent runs and the descriptive statistics are gathered.

1) RESULTS OF THE FIRST EXPERIMENT

Table 4 depicts the gathered descriptive statistics which are the best, worst, mean, and standard deviation (Std.) of the obtained 3D coverage percentages. As observed, the performance of the proposed algorithm is significantly superior compared to other algorithms.

In particular, CMPA is able to reach 100% coverage for all test cases with lower Std. In addition, the worst coverage obtained by CMPA still the best compared to other comparators. It is also clear that the performance of the proposed algorithm is stable while changing the testing environment. Moreover, the obtained results of CMPA and the other compared algorithms are analyzed with the Friedman Rank test [33] with a level of confidence that equals 0.05. Fig. 6 shows the ranked mean values of the Friedman Rank test for the five large-scale test cases. As observed, the rank of the proposed algorithm is significantly greater than other compared algorithms with a p-value equals to zero. This means that the obtained coverage percentages of CMPA are considerably greater than the comparators.

TABLE 4. Descriptive statistics of CMPA and the comparators for the first experiment.

Cases	Algorithms	Worst	Best	Mean	Std.
Case 1	CMPA	**99.40%**	100.00%	**99.90%**	**0.176**
	COA	75.88%	97.16%	89.34%	4.498
	HHO	75.36%	99.24%	91.57%	5.822
	SMA	83.96%	98.84%	92.43%	3.963
	LFD	83.16%	95.04%	88.21%	2.733
	SSA	96.00%	100.00%	98.80%	1.087
	WOA	83.00%	97.76%	92.56%	3.868
Case 2	CMPA	**97.50%**	**100.00%**	**99.33%**	**0.690**
	COA	71.78%	82.28%	77.50%	2.896
	HHO	76.25%	89.00%	80.96%	3.269
	SMA	61.44%	80.94%	71.56%	5.060
	LFD	63.00%	80.56%	68.93%	4.202
	SSA	83.86%	95.83%	92.14%	3.017
	WOA	74.53%	94.61%	84.82%	5.324
Case 3	CMPA	**99.73%**	**100.00%**	**99.95%**	**0.071**
	COA	81.27%	92.98%	85.53%	2.376
	HHO	79.56%	95.27%	88.83%	4.476
	SMA	68.03%	89.59%	79.12%	5.881
	LFD	73.66%	84.64%	77.98%	2.705
	SSA	91.00%	99.47%	97.11%	1.884
	WOA	83.50%	97.97%	91.63%	3.696
Case 4	CMPA	**99.70%**	**100.00%**	**99.96%**	**0.066**
	COA	78.00%	93.19%	86.02%	3.256
	HHO	76.16%	94.20%	85.69%	4.113
	SMA	69.44%	92.70%	78.19%	5.456
	LFD	70.81%	83.05%	76.26%	2.675
	SSA	90.22%	98.89%	96.69%	2.003
	WOA	82.28%	97.33%	91.87%	3.234
Case 5	CMPA	**99.49%**	**100.00%**	**99.91%**	**0.128**
	COA	76.31%	92.42%	82.98%	2.988
	HHO	71.72%	91.50%	83.85%	4.500
	SMA	66.11%	83.35%	74.21%	4.969
	LFD	67.75%	86.03%	74.42%	4.929
	SSA	90.41%	98.74%	95.11%	1.855
	WOA	83.73%	95.34%	89.59%	3.195

TABLE 5. Descriptive statistics of CMPA and the comparators for the second experiment.

Cases	Algorithms	Worst	Best	Mean	Std.
Case R1	CMPA	**91.42%**	**98.01%**	**96.878%**	**1.194**
	PSOGSA	NA	95.87%	NA	NA
	CMA_ES	NA	93.64%	NA	NA
	GWOCS	NA	97.53%	NA	NA
Case R2	CMPA	**95.95%**	**99.98%**	**98.8443%**	**1.01**
	PSOGSA	NA	94.24%	NA	NA
	CMA_ES	NA	60.50%	NA	NA
	GWOCS	NA	99.93%	NA	NA
Case R3	CMPA	**87.31%**	**97.69%**	**93.3268%**	**3.65**
	PSOGSA	NA	NA	NA	7.80
	CMA_ES	NA	NA	NA	NA
	GWOCS	NA	95.81%	NA	NA

NA means not a number.

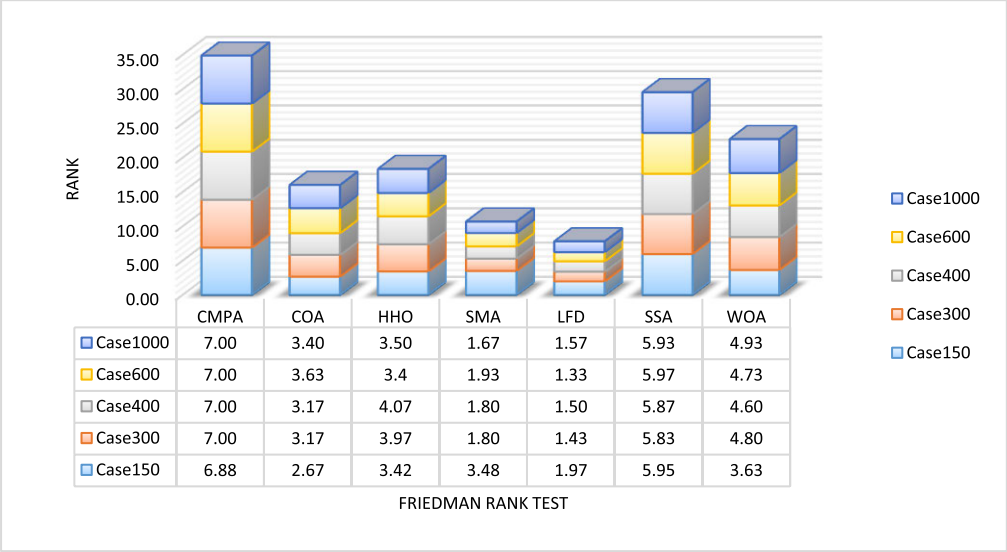

	CMPA	COA	HHO	SMA	LFD	SSA	WOA
Case1000	7.00	3.40	3.50	1.67	1.57	5.93	4.93
Case600	7.00	3.63	3.4	1.93	1.33	5.97	4.73
Case400	7.00	3.17	4.07	1.80	1.50	5.87	4.60
Case300	7.00	3.17	3.97	1.80	1.43	5.83	4.80
Case150	6.88	2.67	3.42	3.48	1.97	5.95	3.63

FIGURE 6. Friedman results for the first test cases.

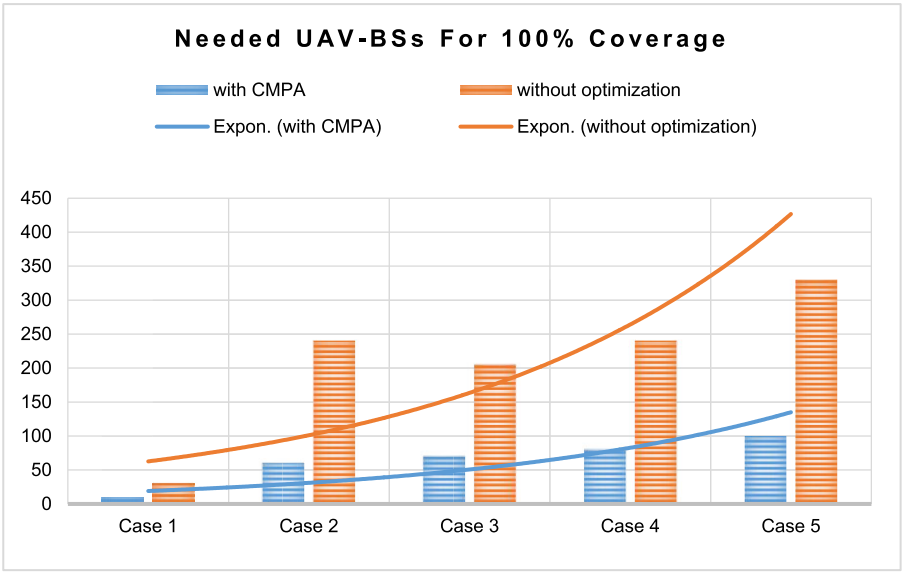

FIGURE 7. Needed UAV- BSs for total coverage in large-scale test cases.

2) RESULTS OF THE SECOND EXPERIMENT

In Table 5, the descriptive statistics of the second experiment are presented. As clearly observed, the proposed algorithm can efficiently maximize the area coverage without constraints violation.

On the other hand, PSOGSA, CMA-ES, and GWOCS are trapped in the infeasible area of solutions even after increasing the population size of CMA-ES.

However the high difficulty of these test cases, the proposed algorithm is able to find the best coverage percentage against other hybrid algorithms. Moreover, CMPA obtained best values are significantly greater than the expected coverage percentages. Also, the CMPA values of Std. denotes its staple performance.

VII. THE IMPLICATION OF CMPA ON COST-EFFICIENT QOS OF 6G TECHNOLOGY

In order to achieve total coverage in vast areas, it may lead to higher setup costs of more UAV-BSs. This mainly shows the importance of using an efficient optimization algorithm for optimizing the spatial distribution of these BSs, especially in large-scale areas. Fig.7 depicts the expected number of needed UAV-BSs for complete coverage with the growth of the covered area. As observed, the usage of CMPA considerably reduces the number of needed UAV-BSs and accordingly reduces costs. On the other hand, not using optimization may lead to a significant cost increment.

There is another effective way for increasing the 6G coverage in large-scale areas. This can be achieved by empowering

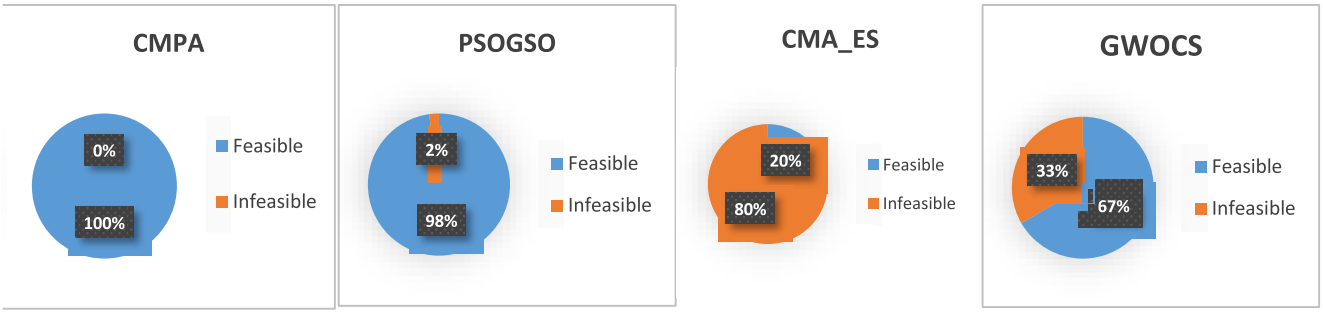

FIGURE 8. The feasibility percentages of CMPA against Comparators.

the system of UAV-BSs with RIS. The spatial allocation of UAV-BSs mainly affects the incident angle between them and RISs and by consequence affects the 6G area coverage. The proposed algorithm can efficiently solve such a problem without constraint violations. Fig.8 shows the feasibility and infeasibility percentages of CMPA and the compared algorithms. As observed, only the proposed algorithm reaches one hundred percent feasibility.

VIII. CONCLUSION AND FUTURE WORKS

The integration of AI and the 3D framework are essential features of 6G wireless networks. In this paper, an enhanced CI optimization algorithm is proposed for finding the best position of UAV-BSs and RIS empowered UAV-BSs in 6G wireless networks. For the first experiment, CMPA is tested on solving many large-scale 3D problems and compared with other recent algorithms. The experimental results indicate the significant efficiency of the proposed algorithm as it achieves a one hundred percent feasible solution of all case studies. For the second experiment, the proposed algorithm is able to find the best coverage percentage for RIS-empowered UAV-BSs in 3D large-scale test cases. Although CMPA is compared with other powerful hybrid algorithms, it significantly achieves the best results without constraint violations. In addition, the cost-efficient QoS of 6G wireless networks is noteworthy improved by the proposed algorithm as it reduces the number of needed UAV-BSs for total coverage.

For future works, we suggest optimizing other 6G functionalities with CMPA such as auto-adjusting radio waves, dynamic allocation of underwater, and sub-band scheduling problems. In addition, we suggest enhancing MPA by the hybridization with other AI techniques such as Fuzzy Logic and Artificial Neural Networks.

REFERENCES

[1] M. Kortas, O. Habachi, A. Bouallegue, V. Meghdadi, T. Ezzedine, and J. P. Cances, "The energy-aware matrix completion-based data gathering scheme for wireless sensor networks," *IEEE Access*, vol. 8, pp. 30772–30788, 2020, doi: 10.1109/ACCESS.2020.2972970.

[2] B. Zong, C. Fan, X. Wang, X. Duan, B. Wang, and J. Wang, "6G technologies: Key drivers, core requirements, system architectures, and enabling technologies," *IEEE Veh. Technol. Mag.*, vol. 14, no. 3, pp. 18–27, Sep. 2019, doi: 10.1109/MVT.2019.2921398.

[3] E. Basar, "Reconfigurable intelligent surface-based index modulation: A new beyond MIMO paradigm for 6G," *IEEE Trans. Commun.*, vol. 68, no. 5, pp. 3187–3196, May 2020, doi: 10.1109/TCOMM.2020.2971486.

[4] S. J. Nawaz, S. K. Sharma, S. Wyne, M. N. Patwary, and M. Asaduzzaman, "Quantum machine learning for 6G communication networks: State-of-the-art and vision for the future," *IEEE Access*, vol. 7, pp. 46317–46350, 2019, doi: 10.1109/ACCESS.2019.2909490.

[5] K. B. Letaief, W. Chen, Y. Shi, J. Zhang, and Y.-J.-A. Zhang, "The roadmap to 6G: AI empowered wireless networks," *IEEE Commun. Mag.*, vol. 57, no. 8, pp. 84–90, Aug. 2019, doi: 10.1109/MCOM.2019.1900271.

[6] H. Yang, A. Alphones, Z. Xiong, D. Niyato, J. Zhao, and K. Wu, "Artificial-intelligence-enabled intelligent 6G networks," *IEEE Netw.*, vol. 34, no. 6, pp. 272–280, Nov./Dec. 2020, doi: 10.1109/MNET.011.2000195.

[7] H. Hashida, Y. Kawamoto, and N. Kato, "Intelligent reflecting surface placement optimization in air-ground communication networks toward 6G," *IEEE Wireless Commun.*, vol. 27, no. 6, pp. 146–151, Dec. 2020, doi: 10.1109/MWC.001.2000142.

[8] Y. Fu, K. N. Doan, and T. Q. S. Quek, "On recommendation-aware content caching for 6G: An artificial intelligence and optimization empowered paradigm," *Digit. Commun. Netw.*, vol. 6, no. 3, pp. 304–311, Aug. 2020, doi: 10.1016/j.dcan.2020.06.005.

[9] A. Tarable, F. Malandrino, L. Dossi, R. Nebuloni, G. Virone, and A. Nordio, "Meta-surface optimization in 6G sub-THz communications," in *Proc. IEEE Int. Conf. Commun. Workshops (ICC Workshops)*, Jun. 2020, pp. 1–6, doi: 10.1109/ICCWorkshops49005.2020.9145267.

[10] M. Yu, A. Tang, X. Wang, and C. Han, "Joint scheduling and power allocation for 6G terahertz mesh networks," in *Proc. Int. Conf. Comput., Netw. Commun. (ICNC)*, Feb. 2020, pp. 631–635, doi: 10.1109/ICNC47757.2020.9049790.

[11] E. Calvanese Strinati, S. Barbarossa, T. Choi, A. Pietrabissa, A. Giuseppi, E. De Santis, J. Vidal, Z. Becvar, T. Haustein, N. Cassiau, F. Costanzo, J. Kim, and I. Kim, "6G in the sky: On-demand intelligence at the edge of 3D networks," *ETRI J.*, vol. 42, no. 5, pp. 643–657, Oct. 2020, doi: 10.4218/etrij.2020-0205.

[12] M. K. Watfa and S. Commuri, "The 3-Dimensional wireless sensor network coverage problem," in *Proc. IEEE Int. Conf. Netw., Sens. Control*, Apr. 2006, pp. 856–861, doi: 10.1109/ICNSC.2006.1673259.

[13] X. Bai, C. Zhang, D. Xuan, and W. Jia, "Full-coverage and k-Connectivity (k=14,6) three dimensional networks," in *Proc. 28th Conf. Comput. Commun.*, Apr. 2009, pp. 388–396, doi: 10.1109/INFCOM.2009.5061943.

[14] T. Andersen and S. Tirthapura, "Wireless sensor deployment for 3D coverage with constraints," in *Proc. 6th Int. Conf. Networked Sens. Syst. (INSS)*, Jun. 2009, pp. 78–81, doi: 10.1109/INSS.2009.5409946.

[15] X. Liu, G. Kang, N. Zhang, B. Zhu, C. Li, Y. Chai, and Y. Liu, "A three-dimensional network coverage optimization algorithm in healthcare system," in *Proc. IEEE 16th Int. Conf. E-Health Netw., Appl. Services (Healthcom)*, Oct. 2014, pp. 323–328, doi: 10.1109/HealthCom.2014.7001862.

[16] D. Sharma and V. Gupta, "Modeling 3D WSN to maximize coverage using harmony search scheme," in *Proc. Adv. Intell. Syst. Comput.*, vol. 949, 2020, pp. 95–111, doi: 10.1007/978-981-13-8196-6_10.

[17] W. Ding, M. Abdel-Basset, K. A. Eldrandaly, L. Abdel-Fatah, and V. H. C. de Albuquerque, "Smart supervision of cardiomyopathy based on fuzzy harris hawks optimizer and wearable sensing data optimization: A new model," *IEEE Trans. Cybern.*, early access, Jun. 24, 2020, doi: 10.1109/TCYB.2020.3000440.

[18] A. Faramarzi, M. Heidarinejad, S. Mirjalili, and A. H. Gandomi, "Marine predators algorithm: A nature-inspired Metaheuristic," *Expert Syst. Appl.*, vol. 152, Aug. 2020, Art. no. 113377, doi: 10.1016/j.eswa.2020.113377.

[19] S. Milner, C. Davis, H. Zhang, and J. Llorca, "Nature-inspired self-organization, control, and optimization in heterogeneous wireless networks," *IEEE Trans. Mobile Comput.*, vol. 11, no. 7, pp. 1207–1222, Jul. 2012, doi: 10.1109/TMC.2011.141.

[20] X. Yuan, Y. J. Angela Zhang, Y. Shi, W. Yan, and H. Liu, "Reconfigurable-intelligent-surface empowered wireless communications: Challenges and opportunities," *IEEE Wireless Commun.*, early access, Feb. 22, 2021, doi: 10.1109/MWC.001.2000256.

[21] M. Di Renzo, K. Ntontin, J. Song, F. H. Danufane, X. Qian, F. Lazarakis, J. de Rosny, D.-T. Phan-Huy, O. Simeone, R. Zhang, M. Debbah, G. Lerosey, M. Fink, S. Tretyakov, and S. Shamai, "Reconfigurable intelligent surfaces vs. Relaying: Differences, similarities, and performance comparison," 2019, *arXiv:1908.08747*. [Online]. Available: http://arxiv.org/abs/1908.08747

[22] S. Li, B. Duo, X. Yuan, Y.-C. Liang, and M. Di Renzo, "Reconfigurable intelligent surface assisted UAV communication: Joint trajectory design and passive beamforming," *IEEE Wireless Commun. Lett.*, vol. 9, no. 5, pp. 716–720, May 2020, doi: 10.1109/LWC.2020.2966705.

[23] T. Xu, J. He, and C. Shang, "Helper and equivalent objectives: Efficient approach for constrained optimization," *IEEE Trans. Cybern.*, early access, Mar. 27, 2020, doi: 10.1109/tcyb.2020.2979821.

[24] J. Pierezan and L. Dos Santos Coelho, "Coyote optimization algorithm: A new metaheuristic for global optimization problems," in *Proc. IEEE Congr. Evol. Comput.*, Sep. 2018, pp. 1–8, doi: 10.1109/CEC.2018.8477769.

[25] A. A. Heidari, S. Mirjalili, H. Faris, I. Aljarah, M. Mafarja, and H. Chen, "Harris hawks optimization: Algorithm and applications," *Future Gener. Comput. Syst.*, vol. 97, pp. 849–872, Aug. 2019, doi: 10.1016/j.future.2019.02.028.

[26] S. Li, H. Chen, M. Wang, A. A. Heidari, and S. Mirjalili, "Slime mould algorithm: A new method for stochastic optimization," *Future Gener. Comput. Syst.*, vol. 111, pp. 300–323, Oct. 2020, doi: 10.1016/j.future.2020.03.055.

[27] E. H. Houssein, M. R. Saad, F. A. Hashim, H. Shaban, and M. Hassaballah, "Lévy flight distribution: A new Metaheuristic algorithm for solving engineering optimization problems," *Eng. Appl. Artif. Intell.*, vol. 94, Sep. 2020, Art. no. 103731, doi: 10.1016/j.engappai.2020.103731.

[28] S. Mirjalili, A. H. Gandomi, S. Z. Mirjalili, S. Saremi, H. Faris, and S. M. Mirjalili, "Salp swarm algorithm: A bio-inspired optimizer for engineering design problems," *Adv. Eng. Softw.*, vol. 114, pp. 163–191, Dec. 2017, doi: 10.1016/j.advengsoft.2017.07.002.

[29] S. Mirjalili and A. Lewis, "The whale optimization algorithm," *Adv. Eng. Softw.*, vol. 95, pp. 51–67, May 2016, doi: 10.1016/j.advengsoft.2016.01.008.

[30] S. Mirjalili and S. Z. M. Hashim, "A new hybrid PSOGSA algorithm for function optimization," in *Proc. Int. Conf. Comput. Inf. Appl.*, Dec. 2010, pp. 374–377, doi: 10.1109/ICCIA.2010.6141614.

[31] R. Biedrzycki, "Handling bound constraints in CMA-ES: An experimental study," *Swarm Evol. Comput.*, vol. 52, Feb. 2020, Art. no. 100627, doi: 10.1016/j.swevo.2019.100627.

[32] W. Long, S. Cai, J. Jiao, M. Xu, and T. Wu, "A new hybrid algorithm based on grey wolf optimizer and cuckoo search for parameter extraction of solar photovoltaic models," *Energy Convers. Manage.*, vol. 203, Jan. 2020, Art. no. 112243, doi: 10.1016/j.enconman.2019.112243.

[33] W. Hernandez, A. Mendez, R. Zalakeviciute, and A. M. Diaz-Marquez, "Analysis of the information obtained from $PM_{2.5}$ concentration measurements in an urban park," *IEEE Trans. Instrum. Meas.*, vol. 69, no. 9, pp. 6296–6311, Sep. 2020, doi: 10.1109/tim.2020.2966360.

MOHAMED ABDEL-BASSET received the B.Sc. and M.Sc. degrees from the Faculty of Computers and Informatics, Zagazig University, Egypt, and the Ph.D. degree from the Faculty of Computers and Informatics, Menoufia University, Egypt. He is currently an Associate Professor with the Faculty of Computers and Informatics, Zagazig University. His research interests include optimization, operations research, data mining, computational intelligence, applied statistics, decision support systems, robust optimization, engineering optimization, multi-objective optimization, swarm intelligence, evolutionary algorithms, and artificial neural networks. He is working on the application of multi-objective and robust metaheuristic optimization techniques. He is also an editor/reviewer in different international journals and conferences. He holds the program chair in many conferences in the fields of decision making analysis, big data, optimization, complexity, and the Internet of Things, and as editorial collaboration in some journals of high impact.

LAILA ABDEL-FATAH received the B.S. and M.Sc. degrees in information systems and decision support from the Faculty of Computers and Informatics, Zagazig University, Egypt. She is currently an Assistant Lecturer with the Faculty of Computers and Informatics, Zagazig University. Her research interests include computation intelligence (CI), fuzzy logic, artificial intelligence (AI), the Internet of Things (IoT), metaheuristic algorithms, geographic information systems (GIS), and spatial optimization.

KHALID A. ELDRANDALY received the Ph.D. degree in systems engineering (GIS). He was a Visiting Scholar with Texas A&M University, USA, for two years. He is currently a Professor of Information Systems, the Dean of Academic Affairs, the Faculty of Computers and Informatics, and the CIO and the Director of the Communication and Information Technology Center, Zagazig University, Egypt. He is also a certified GIS Professional (GISP). His research interests include GIS, expert systems, SDSS, MCDM, and intelligent techniques in decision making. He is a member of the Egyptian Engineers Syndicate, World Academy of Young Scientists (WAY), Arab Union of Scientists and Researchers (AUSR), Texas A&M International Faculty Network, Egyptian Software Engineers Association (ESEA), GIS Certification Institute, International Society for Environmental Information Science, and Association of Computing Machinery (ACM). He is also currently serves as a member in the Review Committee of the IAJIT, IJGIS, IJOPCM, ASOC, ACIT, JEI, FCT, and AJSE.

NABIL M. ABDEL-AZIZ received the M.Sc. and Ph.D. degrees in information systems from the Faculty of Computers and Informatics, Zagazig University. He is currently an Assistant Professor with the Department of Information Systems, Faculty of Computers and Informatics, Zagazig University. He is the Team Leader of Quality Management Unit, Faculty of Computers and Informatics, Zagazig University. His research interests include GIS, spatial decision support systems, multi-criteria decision making, and intelligent techniques in decision making. He is a member of Egyptian Software Engineers Association (ESEA).